Terahertz demonstrations of effectively two-dimensional photonic bandgap structures

Yuguang Zhao and D. Grischkowsky

School of Electrical and Computer Engineering, Oklahoma State University, Stillwater, Oklahoma 74078

Received January 19, 2006; revised February 20, 2006; accepted February 24, 2006; posted March 7, 2006 (Doc. ID 67376)

We demonstrate effectively two-dimensional (2D) terahertz (THz) photonic bandgap (PBG) structures for transverse electromagnetic (TEM) mode propagation within metal parallel plate waveguides (PPWG). The 2D-PBG structures consisting of square arrays of dielectric cylinders were characterized by THz time-domain spectroscopy (THz-TDS). THz photonic bandgaps were observed, as determined by the 160 μm lattice constant, the 65 μm diameter, and the dielectric constant of the cylinders. The experimental measurements were fitted with excellent agreement to 2D theory, confirming that for TEM mode propagation, effectively 2D propagation experiments can be achieved within the bounded space of the PPWG. © 2006 Optical Society of America

OCIS codes: 250.0250, 300.6270.

For some time it has been a challenge to experimentally demonstrate that the parallel plate waveguide (PPWG) can be generalized to enable effectively two dimensional (2D) experimental embodiments within the bounded space formed by the narrow separation between the two parallel metal plates.[1–3] The electromagnetic wave equation, as applied to the PPWG with the plate separation along the y axis, shows that transverse electromagnetic (TEM) mode propagation is preserved with included 2D- (x,z) shaped components.[1–3] This situation holds only for the TEM mode, which has no spatial dependence in the y direction and no cutoff frequency. Within this bounded space, 2D reflective,[2] refractive, and diffractive[3] quasi-optical components have been experimentally demonstrated. The resulting TEM wave propagation is analytically described as a 2D wave propagating in the $x-z$ plane; 2D circular and 2D line waves are analogous to 3D spherical and 3D plane waves. This situation allows for the experimental realization of 2D situations that can only be approximated in free space.

Here we report the adaptation of 3D cylindrical photonic bandgap (PBG) microwave structures[4–6] to operational and effectively 2D-PBG THz structures within the bounded space of the PPWG. This demonstration and the resulting excellent fit with strictly 2D theory provides the best confirmation to date of the accuracy of this effectively 2D embodiment. Our observations of the strongly varying, frequency-dependent transmission through the 2D-PBG structures were fitted with excellent agreement by the transfer matrix method theory[7,8] for 3D infinite cylindrical geometry PBG structures, scaled down in size for terahertz (THz) frequencies. Because of the 2D embodiment within the bounded space, no correction was needed due to the finite thickness. The excellent agreement also confirms the fabrication quality of the 2D-PBG structures.

For our experiments, previously handcrafted macroscopic 3D-PBG microwave structures[4–6] were transformed into microscopic 2D-PBG THz structures by using cleanroom-based lithography to reduce the spatial dimensions by as much as 1/100. The consequent 65 μm diameter, 70 μm high, dielectric cylinders standing on a 160 μm periodic square lattice are shown in Fig. 1. THz time-domain spectroscopy (TDS) characterization from 0.2 to 3 THz of these 2D-PBG structures showed marked frequency dependence of transmission and dispersion, demonstrating photonic bandgaps, notched frequency filtering, and high- and low-pass filtering.

These results can be compared with those of a dielectric PBG structure-filled PPWG,[9] which over a frequency range of 0.2 to 0.4 THz showed PBG features together with an observable defect mode in qualitative agreement with theory. Another comparison involves the PBG response from 0.2 to 3.5 THz of the air-spaced, broken-symmetry photonic PPWG,[10] consisting of one metal plate together with the second plate having a metallic lithographically fabricated PBG surface. This photonic PPWG showed sharp spectral responses in regions as large as 1 THz.

Similar to earlier work,[10] we employ microelectromechanical systems technology[11] to make the high-

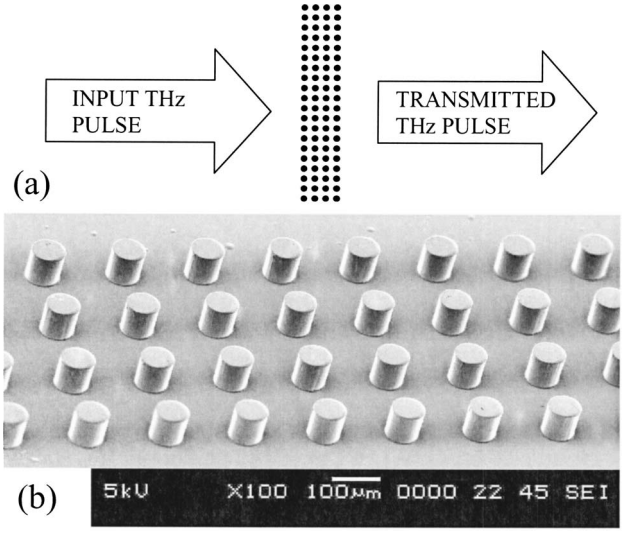

Fig. 1. (a) Schematic diagram showing THz propagation through the columns of the array. (b) Scanning electron microscope (SEM) image of 4-C sample.

quality array shown in Fig. 1(b). However, here we fabricate the dielectric cylinders on the metal-coated surface of a Si wafer to obtain arrays of hard polymer cylinders standing on this metal surface. The resulting processed Si wafer was diced into 25 mm wide $\times 10$ mm long chips to form the lower plate of the waveguide. Four samples with blank, 4-column (4-C), 8-column (8-C), and 60-column (60-C) arrays of cylinders were separately used. Figure 1(b) shows a scanning electron microscope image of the 4-C chip. The 2D-PBG structures were completed by placing the top Al metal plate over and in contact with the top of the cylindrical array. The 2D-PBG samples consist of a matrix array of M rows with N columns, where $N \ll M$ and $M = (20\ \text{mm}/160\ \mu\text{m}) + 1 = 126$. This number of rows is comparatively quite large, encompassing tens of wavelengths and, thereby, sharpening the spectral response and increasing the dynamic range of the filtering response. The total number of cylinders is $M \times N$. As shown in Fig. 1(a), the THz pulse propagation is perpendicular to the columns of cylinders with the linear polarization parallel to the cylinders. The resulting 2D-PBG structures centered within the 10 mm long PPWGs were characterized by waveguide THz-TDS.[1]

The THz optical arrangement converts the incident 3D plane wave from the THz transmitter into an incident 2D line wave matched to the waveguide and couples the waveguide output 2D line wave into an outgoing 3D plane wave, coupled into the THz receiver. Within the PPWG this situation gives a frequency-independent 2D THz beam divergence $\theta \cong \lambda/d = 0.033$ rad, which is also the angular acceptance of the THz receiver. This narrow acceptance angle is important for the sharp frequency response of our measurements.

Figure 2(a) shows the measured THz reference pulse together with three different sample pulses, which have propagated though the 4-C, 8-C, or 60-C, 2D-PBG structure, respectively. The baselines of the pulses have been offset for clarity. The THz reference pulse was transmitted undistorted through the 25 mm wide $\times$ 10 mm long PPWG with 70 μm plate separation and no 2D-PBG structure in place. The sample pulses were attenuated, reshaped, and developed a low-level ringing structure extending to approximately 20 ps for the 4-C and 8-C pulses and to 100 ps for the 60-C pulse. In addition, the sample pulses show slight propagation delays with respect to the reference pulse, propagating at light speed c. These delays of 0.2 ps for 4-C, 0.39 ps for 8-C, and 2.85 ps for 60-C structures are in excellent agreement with the following argument. Within the 2D-PBG the filling factor F is given by the ratio of the cross-sectional area of a cylinder to the lattice spacing area, $F = (\pi/4)\ (65\ \mu\text{m})^2/(160\ \mu\text{m})^2 = 0.130$. The calculated delay D is then given by $D = N(160\ \mu\text{m})F(n-1)/c$, where $n = 1.7$ is the approximate index of refraction[12] of the cylinders. The calculated values are $D = 0.19$, 0.39, and 2.91 ps for $N = 4$, 8, and 60, respectively. Figure 2(b) shows the 60-C pulse in more detail and presents the complex re-

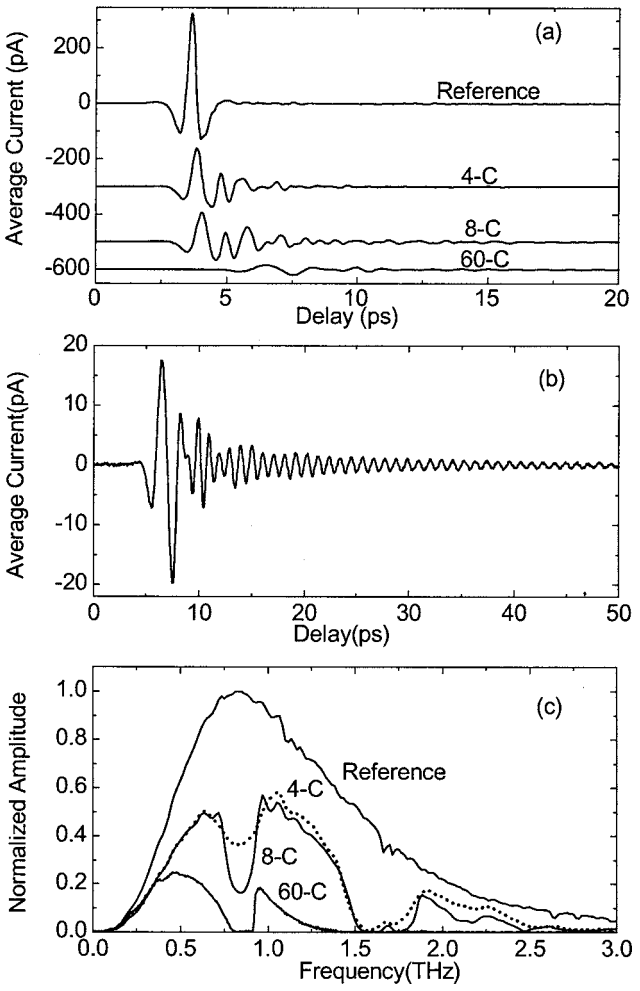

Fig. 2. (a) Measured reference, 4-C, 8-C, and 60-C transmitted THz pulses, respectively. (b) Expanded view of 60-C transmitted pulse. (c) Corresponding amplitude spectra.

shaped waveform with a ringing monotonic decay, measured with a signal-to-noise ratio of approximately 300. Figure 2(c) shows the corresponding amplitude spectra of the reference pulse and the three sample pulses, demonstrating the filtering capability of the 4-C, 8-C, and 60-C structures. The 60-C spectrum is that of the complete pulse extending to 100 ps.

Figure 3(a) shows the corresponding amplitude transmission for all three samples. Well-resolved spectral features are observed that clearly show increasing strength with the number of columns. The 60-C spectrum shows a well-defined PBG from 0.81 to 0.91 THz with a very sharp (0.01 THz) turn on at 0.91 THz. The 8-C transmission shows the same PBG in a developing stage and another developing PBG at higher frequency from 1.5 to 1.84 THz, containing a small relatively sharp transmission peak at 1.70 THz. The amplitudes of the spectral peaks have been reduced by the dielectric absorption of the cylinders.[12]

Figure 3(b) presents the relative phase of the sample pulses with respect to the reference pulse. The dashed lines associated with each sample pulse are the phase shifts Φ determined by the filling factor

time delay, as $\Phi = 2\pi N(160\ \mu\text{m}/\lambda)F(n-1)$. The observable features deviating from the dashed lines describe the phase response associated with 2D-PBG features in the transmission of Fig. 3(a). The large absorption of the 60-C sample truncated the phase determination below 1 THz.

Figure 4 presents the power transmission measurements $T(\omega)$ in dB of the 4-C and 60-C structures, for which $T(\omega) = 20\log|S(\omega)/R(\omega)|$, where $S(\omega)$ is the sample amplitude spectrum and $R(\omega)$ is the reference spectrum. The experimental results are compared with numerical transfer matrix calculations for a 3D infinite cylindrical geometry,[7,8] equivalent to a 2D theory. Based on our THz-TDS measurements of a uniform 90 μm layer of cured Su-8 2025 photoresist data from MicroChem Inc. and previous THz-TDS measurements,[12] the real part of the index of refraction is approximated by $n_r = 1.7$, and the power absorption coefficient $\alpha = 4\pi n_i/\lambda$ is approximated by using the complex index of refraction $n_i = 0.044$. These values determine the dielectric constant $\epsilon = 2.88 + i0.15$, used in the calculation. The comparison with theory gives excellent agreement with the location and depths of the transmission minima for the 4-C sample out to 2 THz. A strong test is that with the same parameters, theory is also in excellent agreement with the 60-C sample for the fast turn-on at 0.91 THz, including the peak height of the transmission and subsequent falloff.

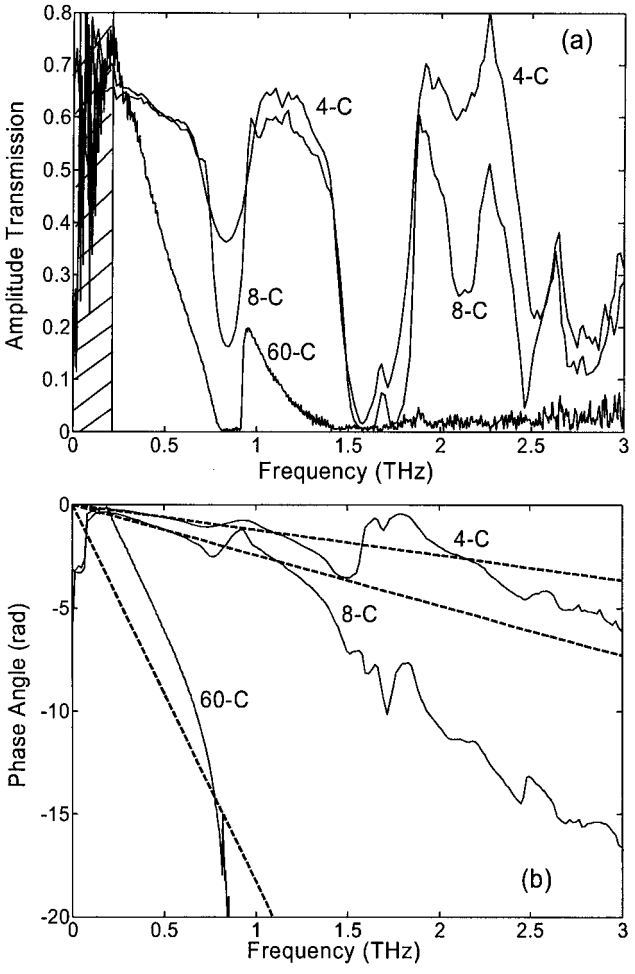

Fig. 3. (a) Measured amplitude transmission of the 4-C, 8-C, and 60-C samples. (b) Measured relative phase.

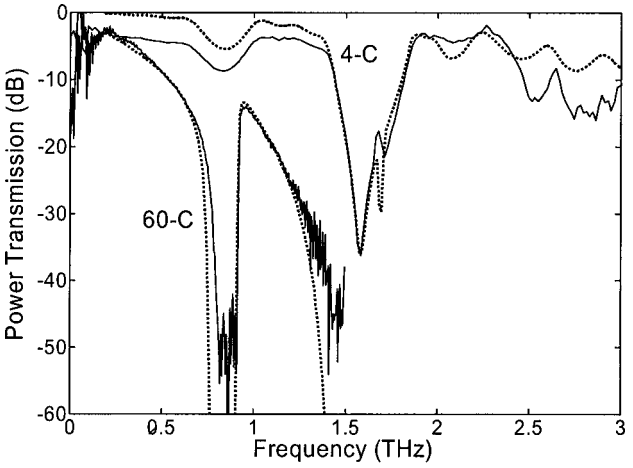

Fig. 4. Measured power transmission for the 4-C and 60-C samples (solid curves) compared with theory (dotted curves).

In summary, we have experimentally demonstrated that the bounded space between the parallel metal plates of a PPWC can be used to create physical embodiments of effectively 2D THz TEM-mode propagation experiments. The measured transmission of such a 2D-PBG frequency filter with a high dynamic range, complicated, and frequency-dependent response was shown to agree with the predictions of 2D theory to exceptional accuracy.

We thank Mufei Gong and Darpan Pradhan for technical support and Adam Bingham for helpful discussions. This research was partially supported by the National Science Foundation. D. Grischkowsky's e-mail address is grischd@ceat.okstate.edu.

References

1. R. Mendis and D. Grischkowsky, Opt. Lett. **26**, 846 (2001).
2. S. Coleman and D. Grischkowsky, Appl. Phys. Lett. **83**, 3656 (2003).
3. J. Dai, S. Coleman, and D. Grischkowsky, Appl. Phys. Lett. **85**, 884 (2004).
4. S. Y. Lin and G. Arjavalingam, J. Opt. Soc. Am. B **11**, 2124 (1994).
5. D. R. Smith, S. Schultz, N. Kroll, M. Sigalas, K. M. Ho, and C. M. Soukoulis, Appl. Phys. Lett. **65**, 645 (1994).
6. S. Y. Lin, V. M. Hietala, and S. K. Lyo, Appl. Phys. Lett. **68**, 3233 (1996).
7. P. M. Bell, J. B. Pendry, L. Martin Moreno, and A. J. Ward, Comput. Phys. Commun. **85**, 306 (1995).
8. Andrew L. Reynolds, Translight Software, University of Glasgow, UK, September 2, 2000.
9. Z. Jian, J. Pearce, and D. Mittleman, Opt. Lett. **29**, 2067 (2004).
10. A. Bingham, Y. Zhao, and D. Grischkowsky, Appl. Phys. Lett. **87**, 051101 (2005).
11. H. Lorenz, M. Despont, N. Fahrni, N. LaBlanca, R. Renaud, and P. Vettiger, J. Micromech. Microeng. **7**, 121 (1997).
12. S. Arscott, F. Garet, P. Mounaix, L. Duvillaret, J.-L. Coutaz, and D. Lippens, Electron. Lett. **35**, 243 (1999).